Photoinduced Hydrogen-Atom Eliminations of 6-Hydroxyquinoline and 7-Hydroxyquinoline Studied by Low-Temperature Matrix-Isolation Infrared Spectroscopy and Density-Functional-Theory Calculations

Masahiko Sekine,[†] Yuko Nagai,[‡] Hiroshi Sekiya,[‡] and Munetaka Nakata*,[†]

Graduate School of BASE (Bio-Applications and Systems Engineering), Tokyo University of Agriculture and Technology, Naka-cho, Koganei, Tokyo 184-8588, Japan, and Department of Chemistry, Faculty of Sciences, Graduate School of Molecular Chemistry, Kyushu University, Hakozaki, Higashi-ku, Fukuoka 812-8581, Japan

Received: April 6, 2009; Revised Manuscript Received: May 26, 2009

Photoreaction mechanisms of 6-hydroxyquinoline (6-HQ) and 7-hydroxyquinoline (7-HQ) in low-temperature argon matrixes have been investigated by Fourier transform infrared (IR) spectroscopy and density-functional-theory (DFT) calculations. A comparison of the observed IR spectra of reactants with the corresponding calculated spectral patterns obtained by the DFT method led to the conclusion that the hydrogen atoms in the O−H group of 6-HQ and in that of 7-HQ are selectively located at the outer position against the quinoline ring. When the matrix samples were irradiated upon UV light around 300 nm, IR spectra of unknown chemical species were observed; they were assigned to the photoreaction intermediates, quinolinoxyl radicals and ketene compounds, produced by eliminations of a hydrogen atom and a hydrogen molecule, respectively. In the photoreaction of 7-HQ, a small amount of keto form was also produced by intramolecular hydrogen-atom transfer from oxygen to nitrogen in an argon cage. Kinetic analyses were made by assuming that 5-ketene and 6-ketene were produced from 6-HQ, while 6-ketene and 7-ketene were produced from 7-HQ. The effective rate constants estimated from the absorbance changes of IR bands against irradiation time revealed that the reaction pathway to produce 6-ketene was minor in both HQs, leading to the conclusion that the conformation of reactants, HQs, plays an important role in the photoproduction of ketenes through biradicals in the Wolff rearrangement.

1. Introduction

Hydroxyquinoline (HQ) has seven structural isomers according to the position of the hydroxy (OH) group bonded to the quinoline ring. It has long been known that the keto−enol isomerization of HQs occurs through intermolecular proton transfer because HQs have both an acid OH group and a basic nitrogen atom on the quinoline ring. The relative stability between the keto and enol forms in aqueous solutions was investigated, resulting in that the stable form, keto or enol, depends on the position of the OH group. For example, the keto form of 2-HQ or 4-HQ, the OH group of which is bonded to the pyridine ring, is more stable than the enol form, in contrast to that the enol form of the other HQs, the OH group of which is bonded to the benzene ring, is more stable than the keto form, including 3-HQ.[1]

The isomerization from the enol form to the keto form of 6-HQ and 7-HQ has been studied by many research groups[2−14] in organic solutions,[2−4,6−8,13,14] solid inert gases,[9−11] and supersonic jets,[5,12] where much attention has been focused on intermolecular interactions and proton transfer. For example, Itoh et al.[3] studied the isomerization of 7-HQ in alcohol solutions at room temperature by time-resolved absorption and fluorescence spectroscopy and reported that the keto form was produced from the enol form by UV irradiation and immediately returns to the enol form through thermal isomerization. The isomerization mechanism proposed was that the keto form is produced by transfer of the hydrogen atom in the OH group to the nitrogen atom via two alcohol molecules through a hydrogen-bonding network upon UV irradiation.

The isomerization from the enol form to the keto form of 7-HQ was also studied at low-temperature matrixes by several groups. Lavin and Collins[9,11] isolated 7-HQ molecules with alcohol in solid inert gases and found that the fluorescence spectra changed with the concentration of alcohol. They assumed that the keto form was produced from the enol form by interacting with two alcohol molecules through intermolecular hydrogen bonding at 10 K. In addition, they isolated 7-HQ molecules without alcohol in solid argon and suggested from the fluorescence spectra that the keto form was also produced from a cyclic dimer.[10] However, the condition of matrix isolation in their experiments was incomplete, and their observed fluorescence around 400 nm was probably due to some aggregates, judging from a recent result obtained by Miura et al.,[13] who concluded from the changes in the UV−visible absorption spectra at various temperatures that keto aggregates produced from the enol monomers of 7-HQ in saturated hydrocarbon solvents frozen at 77 K were stabilized by electrostatic interactions more effectively than by intermolecular hydrogen bonding.

In spite of all these studies by electronic spectroscopy, photoinduced isomerization from the enol form to the keto form of 6-HQ and 7-HQ has not yet been fully elucidated, because the intermolecular interactions at low temperature are complicated and information from electronic spectroscopy is insufficient for determining the geometric structures of relevant chemical species. Thus the following question has been raised:

* Corresponding author. Telephone/fax: +81-42-388-7909. E-mail: necom816@cc.tuat.ac.jp.
[†] Tokyo University of Agriculture and Technology.
[‡] Kyushu University.

10.1021/jp903146v CCC: $40.75
Published on Web 07/01/2009

Does the isomerization from the enol form to the keto form occur due to *intramolecular* hydrogen-atom transfer in isolated states with no *intermolecular* interaction between HQ molecules in aggregation or that between an HQ molecule and solvent molecules in solutions? If not, what kinds of chemical reactions, such as elimination of hydrogen atoms, occur upon electronic excitation by UV irradiation?

The present study is aimed at providing some clues to these questions. We have investigated the photoreaction mechanisms of 6-HQ and 7-HQ by low-temperature matrix-isolation infrared (IR) spectroscopy and density-functional-theory (DFT) calculations. No study has yet been reported on the photoreaction mechanisms of HQ molecules in isolated states, to our knowledge.

Low-temperature matrix-isolation IR spectroscopy combined with the DFT calculation, unlike electronic spectroscopy, enables clear-cut determination of geometric structures of chemical species existing in low-temperature matrixes, especially the time changes of the photochemical products caused by UV irradiation.[15−17] The present study intends to clarify the photoreaction pathways of 6-HQ and 7-HQ as precisely as possible by the following processes: (i) analyses of the geometric structures of the reactants, 6-HQ and 7-HQ, especially the position of the hydrogen atom in the OH group around the C−O bond axis, (ii) identification of the radical species produced by elimination of the hydrogen atom in the OH group; (iii) identification of the intermediates produced by elimination of a hydrogen molecule; (iv) determination of the geometric structures of the intermediates; (v) determination of the effective reaction-rate constants from the kinetic analyses of absorbance changes of IR bands upon UV irradiation; and (vi) step-by-step confirmation of the proposed photoreaction mechanism including the reactive species that remained undetectable in the IR spectra. We also discuss the possibilities of the production of dimers and keto isomers in low-temperature argon matrixes. The present work offers a typical study of photoreaction mechanisms along the pathways by tracing the geometric structures of reactants, intermediates, and products.

2. Experimental and Calculation Methods

Samples of 6-HQ (purity >95.0%) and 7-HQ (purity >99.9999%) were purchased from Wako Purity Ltd. and ACROS Organics, respectively, and were used after vacuum distillation at 363 K to remove water and impurities. Each sample placed in a deposition nozzle with a heating system was vaporized at 346 and 358 K for 6-HQ and 7-HQ, respectively. Pure argon (Taiyo Toyo Sanso, 99.9999%) was flowed over the sample, and the flow rate of argon gas was adjusted to obtain sufficient isolation. The mixed gas was expanded through a stainless steel pipe of 1/8 in. in diameter and deposited on a CsI plate, cooled to 20 K by a closed-cycle helium refrigerator unit (CTI Cryogenics, Model M-22), in a vacuum chamber, kept below 1×10^{-5} Pa by rotary and turbomolecular pumps. UV radiation from a superhigh-pressure mercury lamp of 500 W (Ushio, HB-50106AA-A) was used to induce photoreaction, where a water filter was used to remove thermal reactions and short-wavelength cutoff optical filters, UV30, UV32, and UV34 (HOYA), were used to choose irradiation wavelengths. IR spectra of the matrix sample were measured with a Fourier transform infrared (FTIR) spectrophotometer (JEOL, Model JIR-7000). The band resolution was 0.5 cm^{-1}, and the number of accumulations was 64. Other experimental details are reported elsewhere.[18,19]

DFT calculations with the 6-31++G** basis set were carried out using the Gaussian 03 program.[20] Beck's three-parameter hybrid density functional,[21] in combination with the Lee−Yang−Parr correlation functional (B3LYP),[22] was used to optimize the geometric structures and to obtain relative energies and IR spectral patterns. The IGOR program[23] was used to determine effective rate constants from IR absorbance changes against irradiation time by least-squares fitting.

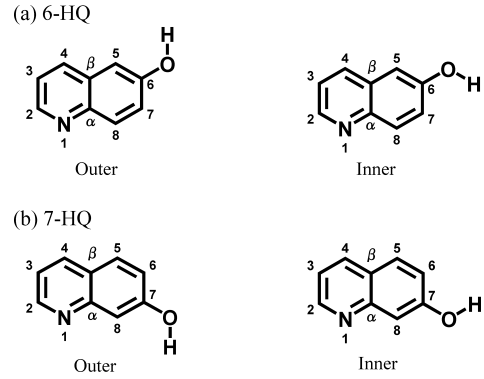

Figure 1. Rotational isomers around the C−O bond axis of 6-HQ and 7-HQ and numbering of atoms.

3. Results and Discussion

Conformation around the C−O Bond Axis of HQs. Two rotational isomers shown in Figure 1 are possible around the C−O bond axis of 6-HQ and 7-HQ. We call them "Outer" and "Inner" hereafter. The hydrogen atom in the OH group for Outer is located far from the molecular long axis, while that for Inner is much closer. Since the geometric structure of Outer is essentially equal to that of Inner except for the position of the hydrogen atom in the OH group, the energy of Outer is expected to be nearly equal to that of Inner. In addition, the potential barrier height around the C−O bond axis between Outer and Inner is expected to be so low that the rotation around the C−O bond axis is nearly free at room temperature; hence it is difficult to distinguish each isomer by normal experimental methods. On the other hand, the technique of low-temperature rare-gas matrix isolation inhibits the thermal rotational motion of the OH group and thus enables independent observation of their IR spectra, from which the conformations can be determined with the aid of DFT calculations.[24,25]

Prior to the experiments of matrix isolation, we performed quantum chemical calculations at the DFT/B3LYP/6-31++G** level to obtain optimized geometries, relative energies, and IR spectral patterns, which resulted in that Outer was more stable than Inner by 1.3 and 4.4 kJ mol^{-1} for 6-HQ and 7-HQ, respectively, after the correction of zero-point vibrational energy. The obtained optimized geometric parameters of 6-HQ and 7-HQ are summarized in Table 1. The C5−C6−O and C7−C6−O bond angles of Outer for 6-HQ are calculated to be 123.5° and 115.8°, which are different from the corresponding values of Inner, 118.1° and 121.3°, respectively. Similar results for the C8−C7−O and C6−C7−O bond angles of 7-HQ are shown in Table 1. The deviations of these values from 120° may be attributed to the interactions between the hydrogen atom in the OH group and a hydrogen atom on the quinoline ring in the neighborhood of the OH group. It is notable that the geometric parameters of Outer for 6-HQ are similar to those of Outer for 7-HQ but differ from those of Inner for 6-HQ, implying that the IR spectra of Outer and Inner are distinguishable for each HQ.

Calculated and Observed IR Spectra of HQs. IR spectral patterns of the two rotational isomers, Inner and Outer for 6-HQ,

TABLE 1: Optimized Geometric Parameters of HQs in Units of Angstroms and Degrees[a]

		6-HQ			7-HQ		
		Inner	Outer		Inner	Outer	dimer
bond length	O−H	0.9659	0.9665	O−H	0.9660	0.9668	0.9866
	C−O	1.370	1.369	C−O	1.370	1.368	1.356
bond angle	C6−O−H	110.1	110.1	C7−O−H	110.2	109.9	110.5
	C5−C6−O	118.1	123.5	C8−C7−O	118.1	123.3	122.4
	C7−C6−O	121.3	115.8	C6−C7−O	121.1	115.8	117.7
	C5−C6−C7	120.5	120.7	C8−C7−C6	120.8	120.9	119.8
dihedral angle	C5−C6−O−H	180.0	0	C8−C7−O−H	180.0	0	24.5
	N−Cα−C8−C7	180.0	180.0	N−Cα−C8−C7	180.0	180.0	169.4

[a] Numbering of atoms is given in Figure 1.

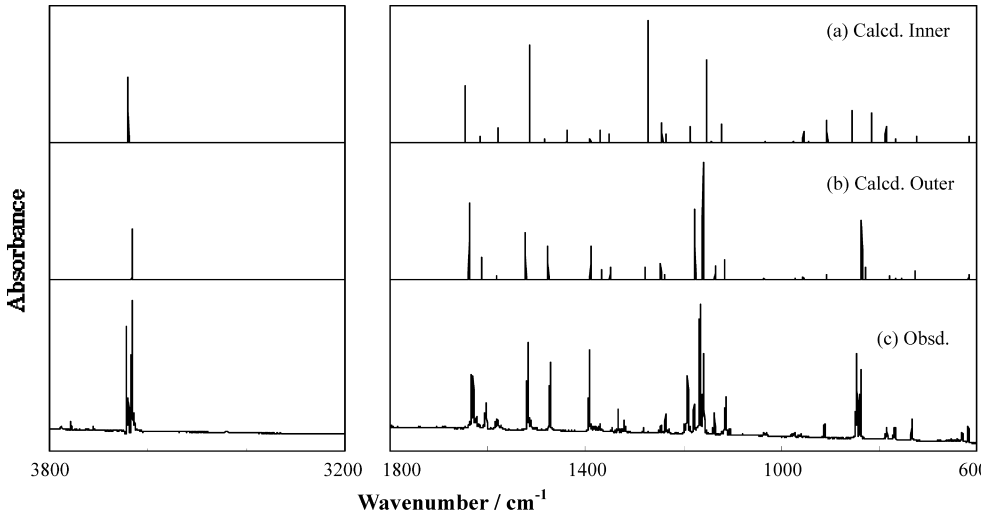

Figure 2. Observed and calculated IR spectra of 6-HQ. Spectral patterns of (a) Inner and (b) Outer, calculated at the DFT/B3LYP/6-31++G** level, where scaling factors of 0.95 and 0.98 are used in the regions higher and lower than 3000 cm^{-1}, and (c) observed matrix-isolation spectrum before UV irradiation.

obtained by the DFT method are shown in Figure 2a,b, where scaling factors of 0.95 and 0.98 are used for IR bands in the regions higher and lower than 3000 cm^{-1}, respectively, to correct anharmonicity of molecular vibrations. It is found, as expected, that the strong characteristic bands of Outer are different from those of Inner. For example, the strong bands of Outer appearing at 1639, 1523, 1176, and 1160 cm^{-1} are due to two quinoline-ring stretching, C−O stretching, and C−O−H bending modes, while the corresponding bands of Inner appear at 1646, 1515, 1272, and 1152 cm^{-1}, respectively. In addition, the spectral pattern of Outer in the region between 700 and 1000 cm^{-1} is totally different from that of Inner as shown in Figure 2a,b, where one strong band appears at 835 cm^{-1} for Outer, in contrast to four or five medium bands for Inner appearing in the same region.

Similarly, the calculated spectral patterns of Inner and Outer for 7-HQ are compared with each other in Figure 3a,b. The wavenumbers and intensities of the vibrational modes associated with the local structure of the C−O−H group differ from each other. One of the most characteristic modes is the C−O stretching mode, which is calculated to be 1178 and 1281 cm^{-1} for Outer and Inner, respectively. This large difference of about 100 cm^{-1} suggests that the existence of Outer and/or Inner in low-temperature argon matrixes can be solved by observation of the IR bands due to this mode.

A spectrum of 6-HQ in an argon matrix measured prior to UV irradiation is compared with the calculated spectral patterns for Inner and Outer in Figure 2. Most of the observed bands, including one appearing in the O−H stretching region around 3600 cm^{-1}, show splitting due to matrix-site effects or Fermi resonance, which are frequently observed in matrix-isolation IR spectra of aromatic compounds containing OH groups such as hydroquinone derivatives.[26,27] The strong bands observed at (1634 and 1630), (1520, 1518, and 1512), (1191 and 1179), and (1168, 1166, and 1159) cm^{-1} for 6-HQ correspond to those of Outer calculated at 1639, 1523, 1176, and 1160 cm^{-1}. The observed bands at (849, 847, and 845) cm^{-1} correspond to that of Outer for the out-of-plane C−H bending mode calculated at 835 cm^{-1}. In contrast to these findings, no band corresponding to the C−O stretching mode of Inner is observed. Therefore, we conclude that only Outer exists in low-temperature argon matrixes. The observed and calculated wavenumbers and relative intensities for Outer of 6-HQ are summarized in Table 2.

A similar discussion is possible when the observed IR spectrum of 7-HQ is compared with the calculated spectral patterns of Inner and Outer. The bands observed at (1635 and 1629), (1522, 1520, and 1516), (1190, 1173, 1170, 1168, and 1166), and (1160 and 1155) cm^{-1} correspond to the calculated strong bands of Outer at 1638, 1524, 1178, and 1156 cm^{-1}, respectively, as shown in Figure 3. In contrast, the most characteristic band due to the C−O stretching mode of Inner is not observed around 1281 cm^{-1}. Therefore, we conclude that only Outer of 7-HQ exists in low-temperature argon matrixes, like 6-HQ. The observed and calculated wavenumbers and relative intensities are summarized in Table 3.

Possibility of Dimer for 7-HQ. The existence of a dimer for 7-HQ in a low-temperature argon matrix was once suggested by Lavin and Collins.[10] They observed three emission bands in a fluorescence excitation spectrum of 7-HQ in matrixes and concluded that one of them was assignable to a cyclic keto

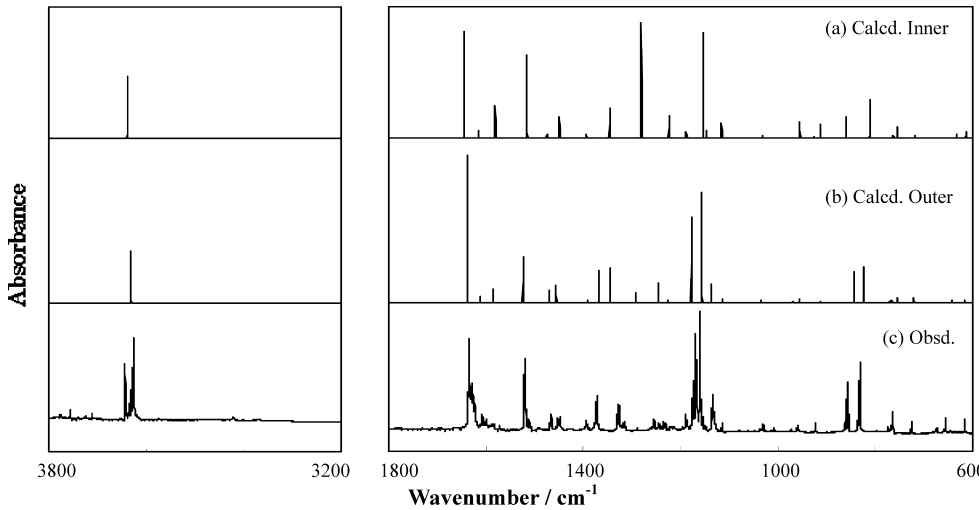

Figure 3. Observed and calculated IR spectra of 7-HQ. Spectral patterns of (a) Inner and (b) Outer, calculated at the DFT/B3LYP/6-31++G** level, where scaling factors of 0.95 and 0.98 are used in the regions higher and lower than 3000 cm^{-1}, and (c) observed matrix-isolation spectrum before UV irradiation.

TABLE 2: Observed and Calculated Wavenumbers of Outer Isomer for 6-HQ

Obsd.		Calcd.[a]		Obsd.		Calcd.[a]	
ν /cm^{-1}	Int.[b]	ν /cm^{-1}	Int.[c]	ν /cm^{-1}	Int.[b]	ν /cm^{-1}	Int.[c]
3644	vs	3633	43	1117	m		
3632	vs			1113	m	1116	17
				1105	w		
1634	m	1639	65	1035	w	1034	1
1630	m			1029	w		
1603	m	1613	19	979	w	971	1
1581	w	1583	3	973	w		
1520	m	1523	41	—		961	0
1518	s			964	w	955	2
1512	w			960	w		
1475	m	1476	28	—		937	0
1472	s			913	w	906	4
—		1448	0	911	w		
1392	s	1390	27	849	m		
1372	w	1367	8	847	m	835	51
1346	w	1350	10	845	s		
1333	m			841	m	828	10
1321	w			838	m		
1281	w	1279	11	837	s		
1246	w	1246	14	788	w	777	4
1237	m	1238	4	785	w		
1229	w			783	w		
1191	m	1176	60	779	vw	766	1
1179	m			771	w	754	1
1168	vs	1160	100	768	w		
1166	vs			733	w	726	7
1162	m			629	w	627	0
1159	s			617	w	616	4
1139	w	1135	11				
1136	m						

[a] Calculated at the DFT/B3LYP/6-31++G** level. Scaling factors of 0.95 and 0.98 are used in the regions higher and lower than 3000 cm^{-1}, respectively. [b] "vs", "s", "m", "w", and "vw" denote very strong, strong, medium, weak, and very weak intensities, respectively. [c] Relative intensities.

dimer, based on the fact that the emission band was similar to the fluorescence spectrum of a 7-HQ−methanol−methanol complex.[9,11] They also reported that the band intensities of the monomer and the cyclic keto dimer decreased and increased, respectively, when the deposition temperature was elevated above 353 K. If their conclusion is correct, the IR spectra observed in the present study should contain the bands of this dimer, since a solid sample of 7-HQ was heated to 358 K in our experiments. If cyclic keto dimer exists in the matrix, a strong band for the characteristic C═O stretching mode should appear in the region around 1700 cm^{-1}. However, no IR bands were observed in the C═O stretching region of our spectrum, as shown in Figure 3c, even if a lower-wavenumber shift due to intermolecular hydrogen bonding is considered; this implies that no cyclic keto dimer exists in the matrix. The emission band observed by Lavin and Collins is probably due to aggregates of more than two molecules, as pointed out by Miura et al.[13]

One may consider a *cyclic enol dimer* as another possible dimer instead of a *cyclic keto dimer*, because it is stabilized by two intermolecular hydrogen bonds between the OH group of one enol and the nitrogen atom of the other enol. Thus we attempted geometric optimization for a cyclic enol dimer by the DFT method. In the calculated optimized geometric structure of a cyclic enol dimer of 7-HQ, displayed in Figure 4, the intermolecular distance between the hydrogen atom in the OH group and the nitrogen atom is calculated to be 2.04 Å. This cyclic enol dimer is found to be more stable than the cyclic

TABLE 3: Observed and Calculated Wavenumbers of Outer Isomer for 7-HQ

Obsd.		Calcd.[a]		Obsd.		Calcd.[a]	
ν /cm^{-1}	Int.[b]	ν /cm^{-1}	Int.[c]	ν /cm^{-1}	Int.[b]	ν /cm^{-1}	Int.[c]
3643	s	3631	36	1190	w		
3626	s			1173	m		
				1170	s	1178	58
1635	s	1638	100	1168	s		
1629	s			1166	m		
1600	w	1612	4	1160	s	1156	75
1572	w	1586	9	1155	w		
1522	s			1137	w	1138	13
1520	s	1524	31	1134	m		
1516	w			1115	w	1115	3
1466	w	1469	9	1031	w	1036	2
1453	w			973	w	971	1
1451	w	1456	12	958	w	956	3
1448	w			—		951	0
1396	w	1392	2	—		944	0
1393	w			923	w	914	1
1376	w			861	m	844	22
1373	m	1369	22	857	s		
1371	m			833	s	825	24
1329	m			832	s		
1326	m	1345	24	774	w	772	1
1317	w			767	w	766	2
1290	w	1292	7	765	w	755	4
1255	w	1247	14	726	w	720	3
1246	w			674	w	643	2
1236	w	1226	2	656	w		
1231	w			617	w	615	2

[a] See the corresponding footnote in Table 2. [b] See the corresponding footnote in Table 2. [c] See the corresponding footnote in Table 2.

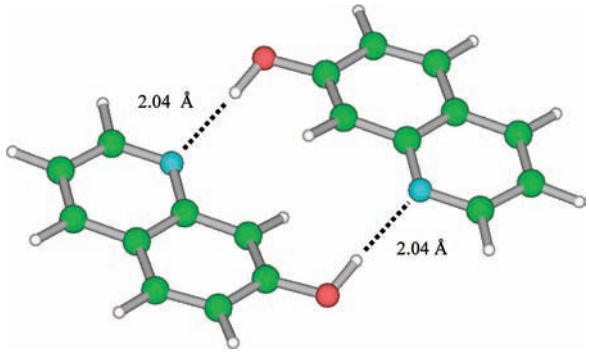

Figure 4. Optimized geometric structure of cyclic enol dimer of 7-HQ. Two monomers are not on the same plane because of repulsion between the two hydrogen atoms bonded to C8.

keto dimer by 132 kJ mol^{-1}. The cyclic enol dimer seems to be more stable than two enol monomers, because the dimer is stabilized by the intermolecular hydrogen bonding between two enol monomers. In fact, the O−H bond in the cyclic enol dimer is calculated to be longer than that in the monomer by 0.02 Å, as shown in Table 1. However, the relative energy of the cyclic enol dimer is calculated to be higher than the sum of two enol monomers by 29 kJ mol^{-1}, although the energy of molecules containing hydrogen bonding may depend on the size of basis sets and/or the calculation methods. This instability may be caused by the steric hindrance between the two hydrogen atoms bonded to C8 of each enol monomer. This interpretation is supported by a comparison of the optimized geometric parameters of the cyclic enol dimer with the corresponding values of the enol monomer (Outer) listed in Table 1 as follows: The dihedral angle of C8−C7−O−H for the enol monomer is 0°, meaning that the OH group is on the plane of the quinoline ring. In contrast, the corresponding dihedral angle for the cyclic enol dimer is 24.5°, which means that two enol monomers forming a cyclic enol dimer are not coplanar. In addition, the dihedral angle of N−Cα−C8−C7 for the enol monomer is 180°, whereas that for the cyclic enol dimer is 169.4°. This distortion of the quinoline ring is certainly caused by the steric hindrance between the two hydrogen atoms bonded to C8 and the hydrogen bonding between the OH group and the nitrogen atom.

To examine the existence of a cyclic enol dimer in low-temperature matrixes, we calculated the IR spectral pattern of the cyclic enol dimer by the DFT method. The characteristic bands associated with the C−O−H bending modes are calculated to be 1259 and 1223 cm^{-1} with a medium intensity, but they are not observed in our spectra. Instead, the corresponding bands for enol monomer are observed at 1178 and 1156 cm^{-1}, respectively. In addition, a strong band of the O−H stretching mode is predicted to appear at 3268 cm^{-1}, being shifted from 3633 cm^{-1} of enol monomer by intermolecular hydrogen bonding between the OH group and the nitrogen atom. However, no strong bands are observed in the region around 3268 cm^{-1}. These findings lead to the conclusion that only enol monomer (Outer) exists in low-temperature matrixes, no cyclic enol dimer, cyclic keto dimer, or any higher aggregates, in the present study.

IR Spectral Changes upon UV Irradiation. When the matrix sample of 6-HQ was exposed to visible light emitted from a superhigh-pressure mercury lamp through a UV34 short-wavelength cutoff filter ($\lambda > 330$ nm), no spectral change was observed. This result is consistent with the previous report on 7-HQ that the 400 nm absorption is due to the keto aggregates instead of the enol monomers.[13] When the cutoff filter was replaced by a UV32 filter ($\lambda > 310$ nm), the intensities of the IR bands of Outer decreased and certain bands due to new chemical species produced from 6-HQ were observed. A difference spectrum after subtraction from the spectrum for the UV irradiation is shown in Figure 5a; hereafter we abbreviate the spectrum gained by this procedure as the *difference spectrum*. It is found that the strongest band of this product

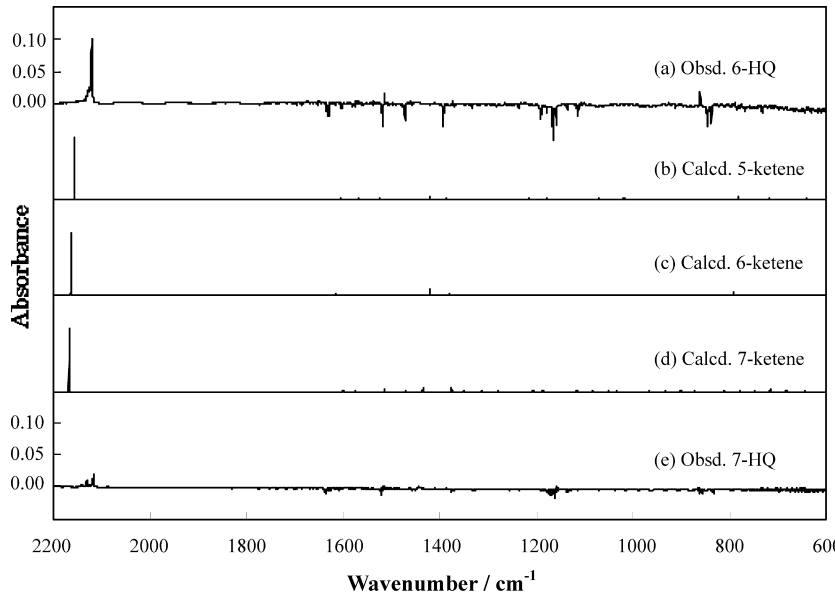

Figure 5. Observed spectral changes and calculated IR spectral patterns of ketenes. (a) Difference spectrum of 6-HQ: after subtraction from the spectrum for 30-min UV irradiation ($\lambda > 310$ nm), calculated spectral patterns of (b) 5-ketene, (c) 6-ketene, and (d) 7-ketene, where a scaling factor of 0.98 is used, and (e) difference spectrum of 7-HQ, 30-min UV irradiation ($\lambda > 310$ nm).

SCHEME 1

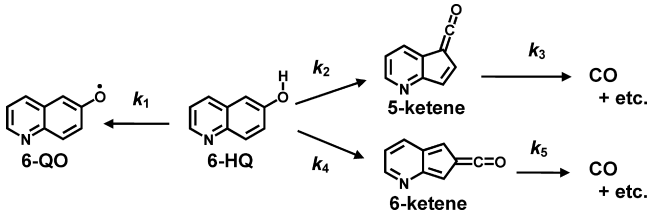

SCHEME 2

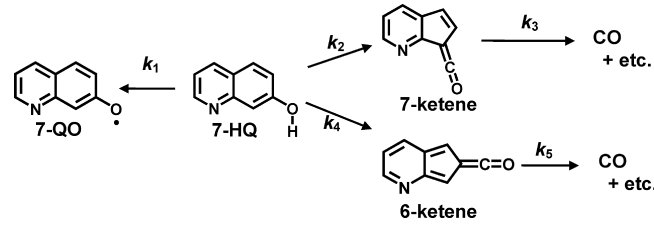

SCHEME 3

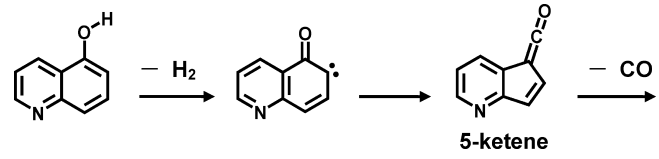

appears at 2121 cm^{-1} in the region of the C═C═O stretching mode of ketene compounds or carbon monoxide (CO).

Cyclopentadienyl ketene is known to be produced from 2-halogenated phenols or α-diazoketo compounds upon UV irradiation.[28−32] In the proposed mechanisms of production, a biradical species, keto carbene, is first produced by the elimination of either hydrogen halide (HX) or nitrogen molecule (N_2), and cyclopentadienyl ketene is generated by the Wolff rearrangement, and then by absorption of the second photon CO is detached from cyclopentadienyl ketene.[30] If a similar photoreaction of 2-halogenated phenols or α-diazoketo compounds occurs in HQs, a similar ketene may be produced by the elimination of a hydrogen molecule (H_2) instead of HX or N_2. As for the photoreaction of 6-HQ, there are two possible hydrogen atoms on the quinoline ring in the neighborhood of the O−H group to make up a detached H_2; one is bonded to C5 and the other is bonded to C7. This means that two kinds of biradicals are produced by elimination of H_2, resulting in two ketene compounds, 5-ketene and 6-ketene denoted in Scheme 1, that can be produced from the corresponding biradicals. In addition, CO may be detached from 5-ketene and/or 6-ketene upon UV irradiation by absorption of the second photon. Then the candidate(s) of the band of the photoproducts for 6-HQ observed at 2121 cm^{-1} may be 5-ketene, 6-ketene, or CO. The calculated spectral patterns of 5-ketene and 6-ketene obtained by the DFT calculation are shown in Figure 5b,c. We will describe the credible assignments on this photoproduct band in the next section.

A similar difference spectrum for 7-HQ is shown in Figure 5e. It is found that the absorbance changes of the reactant and photoproduct bands are smaller than those of 6-HQ shown in Figure 5a, implying that the reactivity of 7-HQ upon the UV irradiation is lower than that of 6-HQ. The two bands are barely observed in the region of ∼2120 cm^{-1}. They are assignable to CO, 6-ketene, and/or 7-ketene, which are possibly produced from 7-HQ by the elimination of H_2 via the corresponding biradicals by the Wolff rearrangement, as shown in Scheme 2.

Identification of Ketenes. The calculated spectral patterns of 5-ketene, 6-ketene, and 7-ketene obtained by the DFT method are compared with the observed difference spectra for 6-HQ and 7-HQ in Figure 5. In all ketenes, the band intensity of the C═C═O stretching mode is exceedingly stronger than the other modes. In contrast, the intensities of the bands appearing in the region between 600 and 1800 cm^{-1} are too weak to be usable for identification of ketenes. To assign the observed bands in the region of the C═C═O stretching mode, we performed a similar experiment using a sample of 5-HQ (purity >96.0%), purchased from Wako Purity Ltd. If a similar photoreaction occurs in 5-HQ, only 5-ketene can be produced by UV irradiation since only the hydrogen atom bonded to C6 in the neighborhood of the OH bond can be eliminated, as shown in Scheme 3; this suggests that a band of ketene appearing in common in the spectra of the photoproducts for 5-HQ and 6-HQ is assignable to 5-ketene.

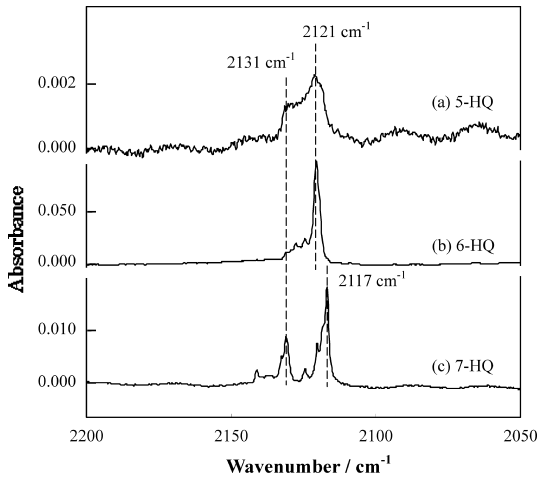

Figure 6. Comparison of spectral changes of 5-HQ, 6-HQ, and 7-HQ upon 30-min UV irradiation ($\lambda > 310$ nm) in the region between 2050 and 2200 cm^{-1}.

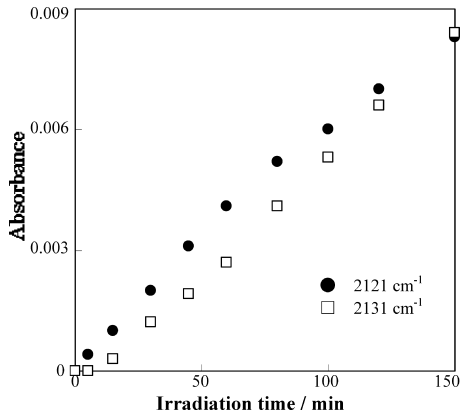

Figure 7. Absorbance changes of IR bands of photoproducts of 5-HQ against UV irradiation time. Closed circles and open squares represent the IR bands at 2121 and 2131 cm^{-1}, respectively. Since the band at 2131 cm^{-1} shows an induction period, it is assigned to the CO fragment detached from 5-ketene.

The observed difference spectra in the region between 2050 and 2200 cm^{-1} for 5-HQ, 6-HQ, and 7-HQ are compared with each other in Figure 6, where their vertical axes are enlarged by suitable factors so as to be comparable. In the spectrum of the photoproducts for 5-HQ, a main peak and a shoulder peak are observed at 2121 and 2131 cm^{-1}, respectively. These bands are not attributed to the site effect, since ketene has no O−H group. One is assignable to 5-ketene, and the other is assignable to CO because no other ketenes can be produced from 5-HQ.

To discriminate CO from 5-ketene, we examined the absorbance changes of the two IR bands against irradiation time. Since CO is produced from 5-ketene, the absorbance change of the IR band for CO should behave like the final product produced via an intermediate, 5-ketene, showing an induction period. Figure 7 shows the absorbance changes of the 2121 and 2131 cm^{-1} bands. The 2131 cm^{-1} band, represented by open squares, shows a clear induction period. Therefore, we assign the shoulder band appearing at 2131 cm^{-1} to CO and the strong band appearing at 2121 cm^{-1} to 5-ketene.

If the above assignments are valid, we can also assign the product bands of 6-HQ; the strong band appearing at 2121 cm^{-1} in Figure 6b is due to 5-ketene. The band of CO is also observed as a shoulder band at 2131 cm^{-1}, although this band is much weaker than that of 5-ketene. This finding suggests that 5-ketene is easily produced from 6-HQ but is hardly destroyed to yield CO by absorption of the second photon, as explained in the section Photoreaction Mechanism of 7-HQ.

In the spectrum of photoproducts of 7-HQ, two main bands are observed at 2117 and 2131 cm^{-1}, as shown in Figure 6c. The 2131 cm^{-1} band can be assigned to CO by comparison with the results of 5-HQ and 6-HQ, while the 2117 cm^{-1} band is assignable to either 6-ketene or 7-ketene. Since 6-ketene is not observed in the spectrum of 6-HQ, we assume that the 2117 cm^{-1} band is due to 7-ketene. Our assignments are further confirmed in the section Photoreaction Mechanism of 7-HQ. Other weak bands appearing in Figure 6 may be due to a CO complex with coproducts, although their amounts are negligible in the kinetic analysis described in the section Photoreaction Mechanism of 7-HQ.

Identification of Qunolinoxyl Radical and Keto Isomer. To identify the chemical species produced from 6-HQ in the 600−1800 cm^{-1} region, we carried out another experiment by using a UV30 filter ($\lambda > 290$ nm) instead of UV32 ($\lambda > 310$ nm) to accelerate the photoreaction. As shown in Figure 8, the difference spectrum facilitates detection of the product bands due to 5-ketene marked with asterisks, while the medium bands at 1514 and 860 cm^{-1} are inconsistent with any calculated bands of 5-ketene and 6-ketene. Similarly, a medium band of the photoproducts of 7-HQ appears at 865 cm^{-1} in the difference spectrum shown in Figure 9. As this band cannot be assigned to either 6-ketene or 7-ketene, we calculated the spectral patterns of possible reaction intermediates to assign these product bands. One of the candidates is quinolinoxyl radical produced by elimination of the hydrogen atom in the OH group of HQs, although no aromatic oxyl radicals have yet been reported. One exception is phenoxyl radical, which is photoproduced from nitrosobenzene, nitrobenzene, or phenol in low-temperature argon matrixes and identified by infrared spectroscopy.[33] If a similar photoreaction of phenol occurs in HQs, quinolinoxyl radical must be produced, as shown in Schemes 1 and 2, but this chemical species has never been studied experimentally and theoretically, to our knowledge. We denote these quinolinoxyl radicals produced from 6-HQ and 7-HQ as 6-QO and 7-QO, respectively.

To assign the photoproduct bands of 6-HQ and 7-HQ besides ketenes, the calculated IR spectral patterns of 6-QO and 7-QO obtained by the DFT method are compared with the corresponding observed spectra in Figures 8 and 9. In the calculated pattern of 6-QO, the strong bands appearing at 1583 and 1494 cm^{-1} are the mixed modes of quinoline-ring stretching and C−O stretching, while the 917, 857, and 774 cm^{-1} bands are the quinoline-ring in-plane bending and two C−H out-of-plane bending modes. These bands are consistent with those observed at 1569, 1514, 926, 860, and 777 cm^{-1}. Therefore, we conclude that 6-QO is produced from 6-HQ by elimination of the hydrogen atom in the OH group upon UV irradiation, like the phenoxyl radical produced from phenol. Their wavenumbers and relative intensities are listed in Table 4. Similarly, the calculated spectral pattern for 7-QO satisfactorily reproduces the observed spectrum of the species produced from 7-HQ upon UV irradiation, as shown in Figure 9; their wavenumbers and relative intensities are listed in Table 5.

There still remain a few unassigned bands in the difference spectrum of 7-HQ shown in Figure 9. For example, the photoproduct bands at 1646 and 1633 cm^{-1} are inconsistent with any calculated bands for 7-QO, 6-ketene, and 7-ketene. Since these bands appear in the region of the C═O stretching mode, keto isomer may be produced from enol Outer of 7-HQ upon UV irradiation. Hence we performed a DFT calculation

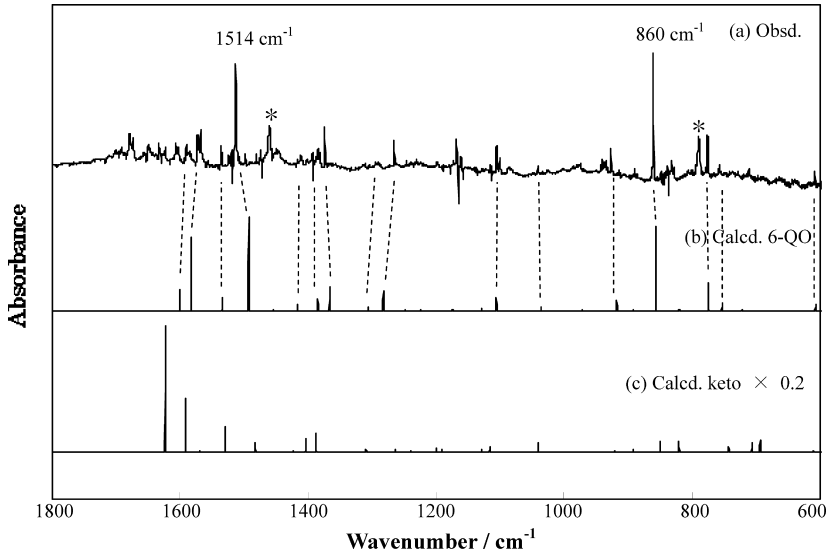

Figure 8. Observed and calculated spectra of photoproducts of 6-HQ. (a) Difference spectrum: after subtraction from the spectrum for 300-min UV irradiation ($\lambda > 290$ nm), where the reactant bands are canceled using a spectrum measured before UV irradiation, (b) spectral pattern of 6-QO radical, and (c) keto isomer of 6-HQ, calculated at the DFT/B3LYP/6-31++G** level, where a scaling factor of 0.98 is used. Bands marked with asterisks (*) are due to 5-ketene. The intensity of keto isomer is multiplied by 0.2.

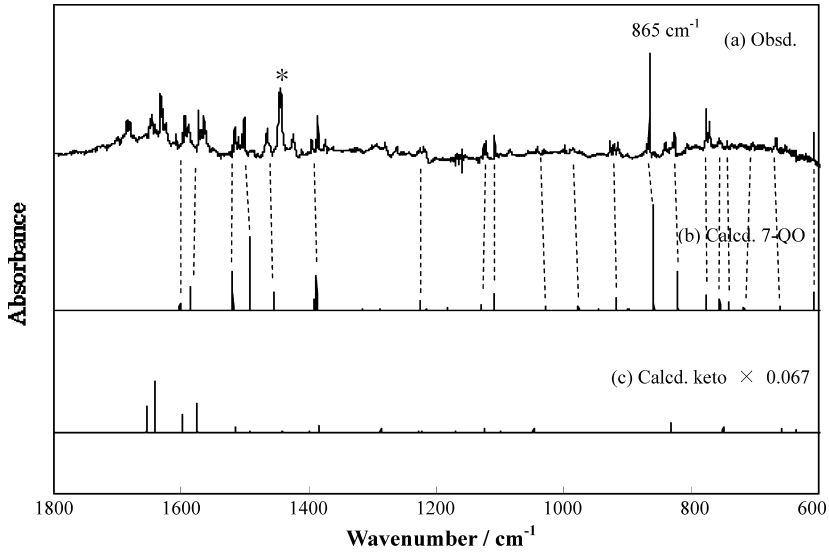

Figure 9. Observed and calculated spectra of photoproducts of 7-HQ. (a) Difference spectrum: after subtraction from the spectrum for 600-min UV irradiation ($\lambda > 290$ nm), where the reactant bands are canceled using a spectrum measured before UV irradiation, (b) spectral pattern of 7-QO radical, and (c) keto isomer of 7-HQ, calculated at the DFT/B3LYP/6-31++G** level, where a scaling factor of 0.98 is used. A band marked with an asterisk (*) is due to 7-ketene. The intensity of keto isomer is multiplied by 0.067.

to obtain the IR spectral pattern of the keto isomer of 7-HQ for comparison with the unassigned product bands. The keto isomer shows the peaks at 1654 and 1642 cm^{-1} for the mixed modes of quinoline-ring stretching and C═O stretching. They are consistent with the observed bands appearing at 1646 and 1633 cm^{-1}, respectively. In addition, the calculated band of the C−H bending mode, 831 cm^{-1}, corresponds to the observed band at 840 cm^{-1}. Therefore, we conclude that the keto isomer is also produced from 7-HQ in addition to 7-QO and 7-ketene. The wavenumbers and relative intensities for the keto isomer of 7-HQ are summarized in Table 6.

Two reaction mechanisms are possible for the isomerization of 7-HQ from the enol form to the keto form. One is *intermolecular* hydrogen-atom transfer between the two monomers in enol dimer. However, this mechanism, proposed by Lavin and Collins,[9] can be excluded because no IR bands of any dimer are observed in the spectrum measured before UV irradiation, as described before. The other mechanism is *intramolecular* hydrogen-atom transfer in an argon cage from the OH group to the nitrogen atom to produce 7-QO. We assume that the hydrogen atom recombines with the nitrogen atom by intramolecular transfer, instead of intermolecular transfer, in an argon cage of the matrix. Once the hydrogen atom is bonded to the nitrogen atom, keto form is produced from 7-QO by electron rearrangement, but the probability of intramolecular hydrogen-atom transfer is so small that the production of keto form is deemed negligible in the kinetic analysis, as described later.

If this mechanism is valid, one would then ask the question of why the keto form of 6-HQ is not produced by intramolecular hydrogen-atom transfer unlike 7-HQ. This may be explained in terms of the distance from the OH group to the nitrogen atom. Note that the OH group in 7-HQ is closer to the nitrogen atom than that in 6-HQ, so that production of

TABLE 4: Observed and Calculated Wavenumbers of 6-QO Radical

Obsd.		Calcd.[a]		Obsd.		Calcd.[a]	
ν/cm^{-1}	Int.[b]	ν/cm^{-1}	Int.[c]	ν/cm^{-1}	Int.[b]	ν/cm^{-1}	Int.[c]
1591	w	1600	23	1106	m	1106	13
1574	m	1583	79	1041	w	1037	4
1569	m			—		981	0
1536	w	1535	14	975	w	972	1
1514	s	1494	100	—		943	0
—		1455	1	926	m	917	11
1412	w	1417	6	890	w	892	1
1385	w	1385	13	860	s	857	90
1374	m	1367	25	832	w	820	1
—		1306	4	777	m	774	29
1266	m	1283	21	757	w	754	8
—		1250	1	—		749	0
—		1224	1	712	w	722	1
—		1174	2	—		638	0
—		1129	2	608	w	608	7

[a] See the corresponding footnote in Table 2. [b] See the corresponding footnote in Table 2. [c] See the corresponding footnote in Table 2.

TABLE 5: Observed and Calculated Wavenumbers of 7-QO Radical

obsd		calcd[a]		obsd		calcd[a]	
ν/cm^{-1}	int[b]	ν/cm^{-1}	int[c]	ν/cm^{-1}	int[b]	ν/cm^{-1}	int[c]
1595	w	1602	7	1031	w	1029	4
1573	m	1586	22	999	w	977	3
1517	w	1519	37	—		969	1
1501	m	1492	70	—		947	1
1467	w	1454	17	927	w	917	12
—		1397	0	900	w	899	2
1396	w	1392	11	865	s	859	100
1385	m	1388	33	826	w	821	37
—		1317	1	776	m	776	15
—		1289	2	757	w	756	10
—		1225	10	744	w	741	8
—		1216	2	—		717	2
—		1182	3	—		662	4
1126	w	1129	6	608	m	608	17
1108	w	1108	16				

[a] See the corresponding footnote in Table 2. [b] See the corresponding footnote in Table 2. [c] See the corresponding footnote in Table 2.

TABLE 6: Observed and Calculated Wavenumbers of Keto Isomer for 7-HQ

obsd		calcd[a]		obsd		calcd[a]	
ν/cm^{-1}	int[b]	ν/cm^{-1}	int[c]	ν/cm^{-1}	int[b]	ν/cm^{-1}	int[c]
3441	w	3437	15	1042	w	1048	7
				—		966	0
1646	m	1654	52	—		935	1
1633	m	1642	100	—		924	1
1589	w	1598	36	—		912	1
1565	m	1575	58	—		896	1
—		1516	12	840	w	831	19
—		1492	4	—		794	0
—		1441	2	—		750	10
—		1398	2	—		749	5
1374	w	1384	14	—		719	0
—		1287	8	—		710	0
—		1275	1	—		658	8
—		1229	2	—		635	5
—		1223	2	—		601	0
—		1170	3	—		525	2
1121	w	1124	8	—		519	4
—		1099	2				

[a] See the corresponding footnote in Table 2. [b] See the corresponding footnote in Table 2. [c] See the corresponding footnote in Table 2.

the keto form of 7-HQ by hydrogen-atom transfer should be much easier than that of 6-HQ. Of course, another reason is that no resonance structures of the keto form of 6-HQ, unlike that of 7-HQ, can be drawn without ion pairs or unpaired electrons.

Photoreaction Mechanism of 6-HQ. It is concluded from the vibrational analyses of the IR spectra measured in low-temperature matrixes that 6-QO and 5-ketene are produced from 6-HQ upon UV irradiation, and then CO is detached from 5-ketene. The reaction pathways for 6-HQ are summarized as follows.

SCHEME 4

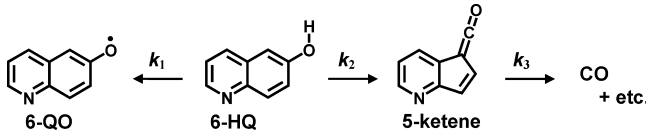

To determine the effective rate constants k_1, k_2, and k_3, for each reaction, we have tried to analyze the IR absorbance changes for each species against UV irradiation time ($\lambda > 310$ nm). The rate equations for each species shown in Scheme 4 are expressed by

$$\frac{da}{dt} = -(k_1 + k_2)a \tag{1}$$

$$\frac{db}{dt} = k_1 a \tag{2}$$

$$\frac{dc}{dt} = k_2 a - k_3 c \tag{3}$$

$$\frac{dd}{dt} = k_3 c \tag{4}$$

where a, b, c, and d represent the amounts of 6-HQ, 6-QO, 5-ketene, and CO, respectively. These rate equations are solved analytically as follows:

$$A = (A_0 - A_\infty)e^{-qt} + A_\infty \tag{5}$$

$$B = \frac{P_1}{q}(A_0 - A_\infty)(1 - e^{-qt}) \tag{6}$$

$$C = \frac{P_2}{q - k_3}(A_0 - A_\infty)(e^{-k_3 t} - e^{-qt}) \tag{7}$$

$$D = \frac{P_3}{q(q - k_3)}(A_0 - A_\infty)\{q(1 - e^{-k_3 t}) - k_3(1 - e^{-qt})\} \tag{8}$$

where A, B, C, and D represent the IR absorbance values of 845 cm^{-1} (6-HQ), 861 cm^{-1} (6-QO), 2121 cm^{-1} (5-ketene), and 2131 cm^{-1} (CO) bands, respectively. Four temporary parameters of $q = k_1 + k_2$, $P_1 = (\varepsilon_B/\varepsilon_A)k_1$, $P_2 = (\varepsilon_C/\varepsilon_A)k_2$, and $P_3 = (\varepsilon_D/\varepsilon_A)k_2$ are used in these equations, where ε_A, ε_B, ε_C, and ε_D represent the absorption coefficients of the corresponding IR bands and A_0 denotes the IR absorbance value of 6-HQ before UV irradiation. As shown in Figure 10a, the IR absorbance of 6-HQ would not approach zero even after infinite time of UV irradiation, implying that some molecules of 6-HQ exist in inactive sites of argon matrix cages, as is well-known in the photoreactions of other molecules in low-temperature matrixes.[34,35] One may consider the possibility of reverse photoreaction to the reactant. However, isomerization from ketene to 6-HQ by the reverse Wolff rearrangement is improbable. Then we define another parameter of the absorbance of inactive 6-HQ as A_∞. Since it is difficult to determine all the parameters of A_0, A_∞, k_1, k_2, k_3, ε_A, ε_B, ε_C, and ε_D from the absorbance changes of A, B, C, and D by a least-squares fitting, the seven parameters A_0, A_∞, q, P_1, P_2, P_3, and k_3, appearing on the right side of eqs 5−8, were determined.

The absorbance changes for 6-HQ, 6-QO, and 5-ketene calculated by using the obtained values reproduce the observed values satisfactorily, but the calculated values for CO, which are displayed by a broken line in Figure 10b, are significantly inconsistent with the corresponding observed values. The induction period for the observed CO band is also less clear than that of CO produced from 5-HQ shown in Figure 7, suggesting that CO is produced not only from 5-ketene but also through another reaction pathway. One of the most probable reaction pathways is that CO is produced from 6-ketene, although no IR bands of 6-ketene are observed in our spectra. If the production rate of 6-ketene is slow and the reaction rate for the detachment of CO from 6-ketene is fast, the lifetime of 6-ketene may be too short for measurement of the IR bands even in low-temperature argon matrixes. Then we assume that 6-ketene is a precursor of CO production as well as 5-ketene, as shown in Scheme 1, where the rate constants of the production and reaction for 6-ketene are defined as k_4 and k_5, respectively. The rate equations for these reaction pathways are expressed by eqs 9−13, where e denotes the amount of 6-ketene.

$$\frac{da}{dt} = -(k_1 + k_2 + k_4)a \tag{9}$$

$$\frac{db}{dt} = k_1 a \tag{10}$$

$$\frac{dc}{dt} = k_2 a - k_3 c \tag{11}$$

$$\frac{dd}{dt} = k_3 c + k_5 e \tag{12}$$

$$\frac{de}{dt} = k_4 a - k_5 e \tag{13}$$

If the steady-state approximation, $de/dt = 0$, is applicable for 6-ketene, the rate eqs 9−13 for the absorbance changes of 6-HQ, 6-QO, 5-ketene, and CO can be solved as follows:

$$A = (A_0 - A_\infty)e^{-qt} + A_\infty \tag{14}$$

$$B = \frac{P_1}{q}(A_0 - A_\infty)(1 - e^{-qt}) \tag{15}$$

$$C = \frac{P_2}{q - k_3}(A_0 - A_\infty)(e^{-k_3 t} - e^{-qt}) \tag{16}$$

$$D = \frac{1}{q}(A_0 - A_\infty)\left\{\frac{P_3}{k_3 - q}(qe^{-k_3 t} - k_3 e^{-qt}) - P_4 e^{-qt} + P_3 + P_4\right\} \tag{17}$$

where five temporary parameters are defined as $q = k_1 + k_2 + k_4$, $P_1 = (\varepsilon_B/\varepsilon_A)k_1$, $P_2 = (\varepsilon_C/\varepsilon_A)k_2$, $P_3 = (\varepsilon_D/\varepsilon_A)k_2$, and $P_4 = (\varepsilon_D/\varepsilon_A)k_4$. The solid lines calculated by using the values of A_0, A_∞, q, P_1, P_2, P_3, P_4, and k_3 determined by a series of least-squares fitting have reproduced all the observed values including CO, as shown in Figure 10.

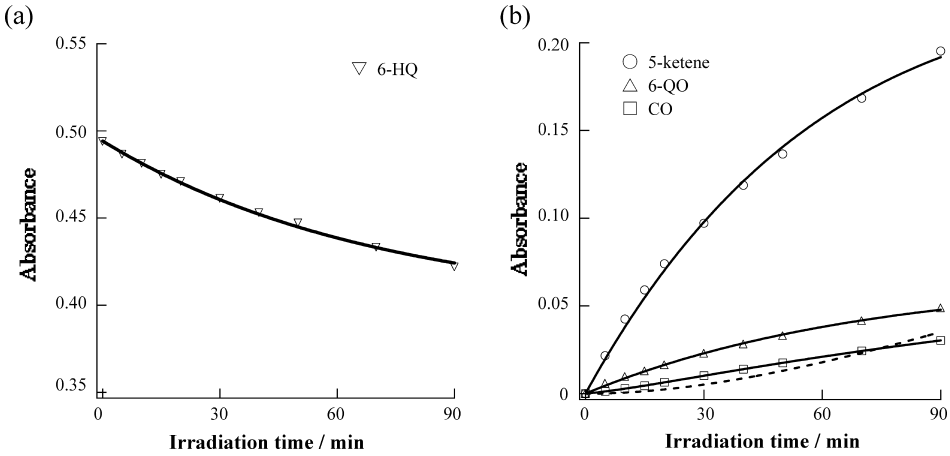

Figure 10. Absorbance changes of the (a) reactant and (b) products of 6-HQ upon UV irradiation. The calculated values for CO obtained using eqs 5−8 without a reaction pathway for the production of 6-ketene, which is drawn by a broken line, is significantly inconsistent with the observed values. The calculated values for all species (solid lines) obtained by least-squares fitting using eqs 14−17 with the condition of steady-state approximation for 6-ketene closely reproduce the observed values.

TABLE 7: Effective Rate Constants upon UV Irradiation (λ > 310 nm) in Units of h^{-1}

	6-HQ	7-HQ
$q = k_1 + k_2 + k_4$	0.85 ± 0.10	0.19 ± 0.10
$P_1 = (\varepsilon_B/\varepsilon_A)k_1$	0.58 ± 0.06	0.15 ± 0.08
$P_2 = (\varepsilon_C/\varepsilon_A)k_2$	2.50 ± 0.19	0.85 ± 0.40
$P_3 = (\varepsilon_D/\varepsilon_A)k_2$	2.10 ± 1.80	1.00 ± 0.68
$P_4 = (\varepsilon_D/\varepsilon_A)k_4$	0.21 ± 0.04	0.13 ± 0.06
k_3	0.09 ± 0.07	0.92 ± 0.16

The coefficients of A_0 and A_∞ are determined mainly from the absorbance changes of 6-HQ to be 0.494 ± 0.001 and 0.397 ± 0.007, respectively, where the uncertainties represent one standard deviation. Other best-fit values are summarized in Table 7. The parameters of P_1, P_2, P_3 and P_4 are only provisional rate constants, because they include absorption coefficients, ε_A, ε_B, ε_C, and ε_D. In other words, the rate constants of k_1, k_2, and k_4 cannot be derived from P_1, P_2, P_3 and P_4 unless the absorption coefficients are determined experimentally. However, the ratio of k_2/k_4 is equal to P_3/P_4, because P_3 and P_4 contain the ratio of absorption coefficients of $\varepsilon_D/\varepsilon_A$ in common. Thus the ratio of P_3/P_4 obtained by the least-squares fitting reveals that k_2 is 10 times larger than k_4, implying that 5-ketene is produced 10 times more easily than 6-ketene. This difference is understandable by the fact that the conformation of 6-HQ in the ground state is Outer in low-temperature matrixes, because, as described above, the hydrogen atom in the OH group is located much closer to the hydrogen atom bonded to C5 than that bonded to C7, as shown in Scheme 1.

We have tried to fit the absorbance changes displayed in Figure 10 by using another reaction scheme that ketenes are produced from 6-QO by elimination of a hydrogen atom, i.e., that 6-QO is a precursor of ketenes. However, the absorbance of 6-QO behaves like a final product instead of an intermediate. On the other hand, 5-ketene never shows any induction periods, implying that 5-ketene is produced from 6-HQ directly by the detachment of H_2. In addition, the calculated values derived from least-squares fitting cannot reproduce the observed absorbance changes. Therefore, we conclude that the two photoreactions to eliminate one hydrogen atom for production of 6-QO and to eliminate H_2 for production of 5-ketene via biradical occur on the different potential surfaces of electronically excited states, for example, a combination of triplet and singlet states. It is reasonable to assume that the hydrogen atom in the OH group interacts with the hydrogen atom bonded to C5 in the neighborhood of the OH group in an electronically excited state upon UV irradiation. In other words, the two hydrogen atoms simultaneously detach from 6-HQ to make H_2. If this is the case, then we can explain the experimental results that 5-ketene is a major product but 6-ketene is only minor.

Photoreaction Mechanism of 7-HQ. A similar kinetic analysis of the photoreaction for 7-HQ has been carried out. The reaction pathways shown in Scheme 2 are used for the kinetic analysis of the absorbance changes against irradiation time, where 6-ketene is assumed to be produced from 7-HQ but immediately detaches CO. As described before, a small amount of the keto form of 7-HQ is also produced. However, the production of keto form is negligible in our kinetic analysis, since its amount is estimated from the IR absorbance to be 1/15 of 7-QO. By using eqs 14−17, and the observed absorbance changes of 832 cm^{-1} (7-HQ), 865 cm^{-1} (7-QO), 2117 cm^{-1} (7-ketene), and 2131 cm^{-1} (CO) bands, the eight parameters are determined by least-squares fitting similar to 6-HQ. The calculated solid lines reproduce the observed absorbance changes for 7-HQ, 7-QO, 7-ketene, and CO as shown in Figure 11, implying that 6-ketene is also produced upon UV irradiation, although no bands of 6-ketene are observed in our spectra. The values of A_0 and A_∞ are determined mainly from the absorbance changes of 7-HQ to be 0.271 ± 0.001 and 0.212 ± 0.028, and other obtained values are summarized in Table 7. It is found from the ratio of P_3/P_4 that 7-ketene is produced 8 times faster than 6-ketene because the hydrogen atom in the OH group of Outer is closer to the hydrogen atom bonded to C8 than that bonded to C6. The explanations presented in the section Photoreaction Mechanism of 6-HQ can be applied to that of 7-HQ.

The parameter of q represents the sum of the reaction rate constants of k_1, k_2, and k_4, i.e., the total reactivity of 7-HQ. The value of q obtained for 7-HQ is 5 times smaller than that for 6-HQ. This is the reason why the absorbance changes for 7-HQ shown in Figure 5e are smaller than those for 6-HQ shown in Figure 5a. This is understandable if the absorption coefficient of 7-HQ for the UV radiation is smaller than that of 6-HQ. Similarly, the rate constant of k_3 represents the reactivity of 5-ketene for 6-HQ or that of 7-ketene for 7-HQ. The value of k_3 obtained for 7-ketene is 10 times larger than that for 5-ketene, demonstrating that CO is produced from 7-HQ mainly via 7-ketene and slightly via 6-ketene. This is the reason why the induction period of CO in the photore-

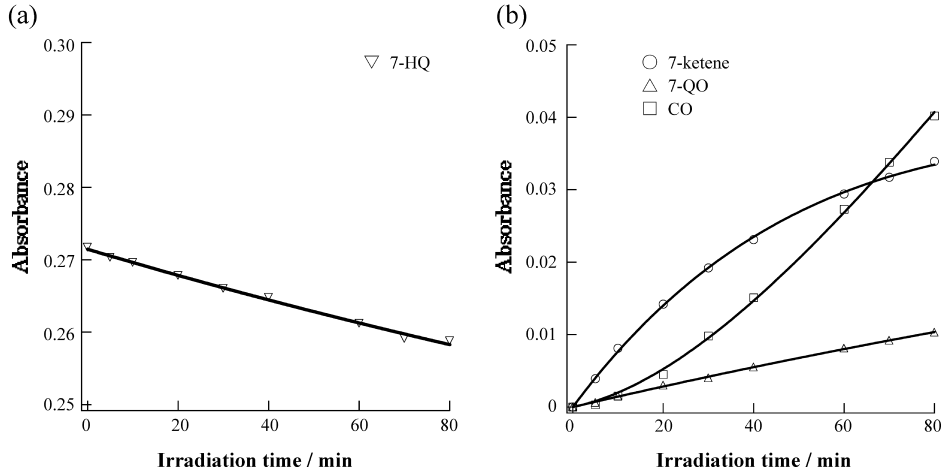

Figure 11. Absorbance changes of the (a) reactant and (b) products for 7-HQ upon UV irradiation. The calculated values for all species obtained by least-squares fittings using eqs 14−17 with the condition of steady-state approximation for 6-ketene, which are drawn by solid lines, closely reproduce the corresponding observed values.

action of 7-HQ is clearer than that in that of 6-HQ, as compared in Figures 10 and 11. This finding is also understandable if the absorption coefficient of 7-ketene for the UV radiation is larger than that of 5-ketene. To confirm these assumptions, UV absorption spectra of HQs and ketenes in low-temperature argon matrixes are valuable. The photochemistry of 7-HQ in a matrix of 2-methyltetrahydrofuran at 77 K studied by fluorescence spectroscopy is reported in detail elsewhere,[36] with two kinds of the observed fluorescence spectra being assignable to keto dimer and 7-QO.

4. Conclusion

The UV-induced photoreaction mechanisms of 6-HQ and 7-HQ have been investigated by low-temperature argon-matrix Fourier transform infrared spectroscopy and quantum chemical calculations. We have found by a comparison of the IR spectra measured before UV irradiation with the calculated spectral patterns that the Outer form, where the hydrogen atom in the OH group is located farther from the molecular long axis, instead of the Inner form exists in low-temperature matrixes in both 6-HQ and 7-HQ. When the matrix samples are exposed to UV light around 300 nm, IR bands for unknown chemical species produced from both HQs are observed; they are identified as QO radical and ketene compounds containing a cyclopentadienyl group. The former is generated from HQ by elimination of the hydrogen atom in the OH group, while the latter is formed by elimination of H_2 composed of the hydrogen atom in the OH group and a hydrogen atom in the neighborhood of the OH group. A small amount of the keto form has been confirmed in the IR spectrum of photoproducts for 7-HQ but not for 6-HQ; this evidences that the keto form is produced by the intramolecular hydrogen-atom transfer in an argon cage, because the distance between O and N for 7-HQ is significantly shorter than that for 6-HQ.

Kinetic analyses were made by assuming that 5-ketene and 6-ketene are produced from 6-HQ, whereas 6-ketene and 7-ketene are produced from 7-HQ. The effective rate constants obtained from the IR absorbance changes against irradiation time by least-squares fitting explain why 5-ketene for 6-HQ and 7-ketene for 7-HQ are produced more easily than 6-ketene. This observation is understandable from the conformation of the hydrogen atom in the OH group of HQs; the hydrogen atom of Outer for 6-HQ is much closer to the hydrogen atom bonded to C5 than that bonded to C7, and the two hydrogen atoms are eliminated as H_2 to generate 5-ketene through biradicals by the Wolff rearrangement. Similarly, the hydrogen atom in the OH group of Outer for 7-HQ is closer to the hydrogen atom bonded to C8 than that bonded to C6, causing easier production of 7-ketene from 7-HQ than of 6-ketene. These findings have led to the conclusion that the two hydrogen atoms of HQs repulsively interact with each other in the ground state but attractively in the electronic state excited by UV irradiation and cause simultaneous detachment of two H atoms as H_2.

Acknowledgment. The authors thank Professor Kozo Kuchitsu (BASE, Tokyo University of A & T) for his helpful discussions. This research was partially supported by a Grant-in-Aid for Scientific Research (c) (No. 19550009) from the Japan Society for the Promotion of Science.

References and Notes

(1) Adrien, A. *Heterocyclic chemistry an introduction*, The Athlone Press, University of London: London, 1959.
(2) Thistlethwaite, P. J.; Corkill, P. J. *Chem. Phys. Lett.* **1982**, *85*, 317.
(3) Itoh, M.; Adachi, T.; Tokumura, K. *J. Am. Chem. Soc.* **1984**, *106*, 850.
(4) Konijnenberg, J.; Ekelmans, G. B.; Huzier, A. H.; Varma, C. A. G. O. *J. Chem. Soc., Faraday Trans.* **1989**, *85*, 39.
(5) Matsumoto, Y.; Ebata, T.; Mikami, N. *J. Phys. Chem. A* **2002**, *106*, 5591.
(6) Bhattacharya, B.; Samanta, A. *J. Phys. Chem. B* **2008**, *112*, 10101.
(7) Mehata, M. S. *J. Phys. Chem. B* **2008**, *112*, 8383.
(8) Mehata, M. S. *Chem. Phys. Lett.* **2007**, *436*, 357.
(9) Lavin, A.; Collins, S. *Chem. Phys. Lett.* **1993**, *204*, 96.
(10) Lavin, A.; Collins, S. *Chem. Phys. Lett.* **1993**, *207*, 513.
(11) Lavin, A.; Collins, S. *J. Phys. Chem.* **1993**, *97*, 13615.
(12) Bach, A.; Tanner, C.; Manca, C.; Frey, H.-M.; Leutwyler, S. *J. Chem. Phys.* **2003**, *119*, 5933.
(13) Miura, M.; Harada, J.; Ogawa, K. *J. Phys. Chem. A* **2007**, *111*, 9854.
(14) Ogawa, K.; Miura, M.; Nakayama, T.; Harada, J. *Chem. Lett.* **2003**, *32*, 840.
(15) Nagaya, M.; Nakata, M. *J. Phys. Chem. A* **2007**, *111*, 6256.
(16) Nishino, S.; Nakata, M. *J. Phys. Chem. A* **2007**, *111*, 7041.
(17) Nishino, S.; Nakata, M. *J. Mol. Struct.* **2008**, *875*, 520–526.
(18) Nagaya, M.; Kudoh, S.; Nakata, M. *Chem. Phys. Lett.* **2006**, *432*, 446.
(19) Yaehata, H.; Nagaya, M.; Kudoh, S.; Nakata, M. *Chem. Phys. Lett.* **2006**, *424*, 279.
(20) Frisch, M. J.; Trucks, G. W.; Schlegel, H. B.; Scuseria, G. E.; Robb, M. A.; Cheeseman, J. R.; Montgomery, J. A., Jr.; Vreven, T.; Kudin, K. N.; Burant, J. C.; Millam, J. M.; Iyengar, S. S.; Tomasi, J.;

Barone, V.; Mennucci, B.; Cossi, M.; Scalmani, G.; Rega, N.; Petersson, G. A.; Nakatsuji, H.; Hada, M.; Ehara, M.; Toyota, K.; Fukuda, R.; Hasegawa, J.; Ishida, M.; Nakajima, T.; Honda, Y.; Kitao, O.; Nakai, H.; Klene, M.; Li, X.; Knox, J. E.; Hratchian, H. P.; Cross, J. B.; Adamo, C.; Jaramillo, J.; Gomperts, R.; Stratmann, R. E.; Yazyev, O.; Austin, A. J.; Cammi, R.; Pomelli, C.; Ochterski, J. W.; Ayala, P. Y.; Morokuma, K.; Voth, G. A.; Salvador, P.; Dannenberg, J. J.; Zakrzewski, V. G.; Dapprich, S.; Daniels, A. D.; Strain, M. C.; Farkas, O.; Malick, D. K.; Rabuck, A. D.; Raghavachari, K.; Foresman, J. B.; Ortiz, J. V.; Cui, Q.; Baboul, A. G.; Clifford, S.; Cioslowski, J.; Stefanov, B. B.; Liu, G.; Liashenko, A.; Piskorz, P.; Komaromi, I.; Martin, R. L.; Fox, D. J.; Keith, T.; Al-Laham, M. A.; Peng, C. Y.; Nanayakkara, A.; Challacombe, M.; Gill, P. M. W.; Johnson, B.; Chen, W.; Wong, M. W.; Gonzalez, C.; Pople, J. A. *Gaussian 03*, revision B.04; Gaussian, Inc.: Pittsburgh, PA, 2003.

(21) Becke, A. D. *J. Phys. Chem.* **1993**, *98*, 5648.

(22) Lee, C.; Yang, W.; Parr, R. G. *Phys. Rev. B* **1988**, *37*, 785.

(23) *IGOR Pro4*, revision 4.0.2.1; Wavemetrics Inc.: Lake Oswego, OR, 2000.

(24) Nagata, M.; Futami, Y.; Akai, N.; Kudoh, S.; Nakata, M. *Chem. Phys. Lett.* **2004**, *392*, 259.

(25) Akai, N.; Kudoh, S.; Takayanagi, M.; Nakata, M. *J. Photochem. Photobiol., A* **2001**, *146*, 49.

(26) Akai, N.; Kudoh, S.; Nakata, M. *J. Photochem. Photobiol., A* **2005**, *169*, 47.

(27) Akai, N.; Kudoh, S.; Takayanagi, M.; Nakata, M. *Chem. Phys. Lett.* **2002**, *356*, 133.

(28) Boule, P.; Richard, C.; David-Oudjehani, K.; Grabner, G. *Proc. Indian Acad. Sci.* **1997**, *109*, 509.

(29) Bonnichon, F.; Richard, C.; Grabner, G. *Chem. Commun.* **2001**, 73.

(30) Akai, N.; Kudoh, S.; Takayanagi, M.; Nakata, M. *Chem. Phys. Lett.* **2002**, *363*, 591.

(31) Bell, G. A.; Dunkin, I. R. *J. Chem. Soc., Faraday Trans. 2* **1985**, *81*, 725.

(32) Tidwell, T. T. *Sci. Synth.* **2006**, *23*, 391.

(33) Spanget-Larsen, J.; Gil, M.; Gorski, A.; Blake, D. M.; Waluk, J.; Radziszewski, J. G. *J. Am. Chem. Soc.* **2001**, *123*, 11253.

(34) Nagashima, N.; Kudoh, S.; Takayanagi, M.; Nakata, M. *J. Phys. Chem. A* **2001**, *105*, 10832.

(35) Minoura, Y.; Nagashima, N.; Kudoh, S.; Nakata, M. J. *Phys. Chem. A* **2004**, *108*, 2353.

(36) Nagai, Y.; Saita, K.; Sekine, M.; Nakata, M.; Nanbu, S.; Sakota, K.; Sekiya, H. To be published.

JP903146V